OPTICAL ACTIVITY OF COMPOUNDS FORMED BY AMINO-COMPLEXES OF Co(III) AND CARBOHYDRATES—I

S. BUNEL* and C. IBARRA

Departamento de Análisis Químico, Facultad de Ciencias Básicas y Farmacéuticas,
Universidad de Chile, Casilla 233, Santiago, Chile

Abstract—The preparation of aminocomplexes of Co(III) containing D-ribose, L-sorbose or D-glucosamine as second ligand is described. Their spectral features and optical activity are reported. Formation in solution of complex species with other chosen carbohydrates gives ground for discussion as to the origin and sign of the observed Cotton effects.

While the formation of complexes by interaction of carbohydrates with metallic ions has been a subject of ever increasing interest,[1] the generation of optically active species has received little attention as compared with other chiral ligands.

We herein report the results of a study which was originally aimed at finding out whether the asymmetric medium provided by a carbohydrate in solution was able to orient the chelate rings of the complex cis-$[Co(phen)_2(H_2O)_2]^{3+}$,[2] (phen = 1,10-phenanthroline), according to a preferred chirality. The presence of a Cotton effect under the Co(III) ion first visible absorption band and the existence of carbohydrate in the compound chromatographically isolated from the reacting mixture revealed that coordination of the carbohydrate to the metallic ion takes place.

Preliminary studies showed that other amino-complexes of Co(III) such as cis-$[Co(en)_2(H_2O)_2]^{3+}$, (en = ethylenediamine),[3] and cis-$[Co(NH_3)_4(H_2O)_2]^{3+}$ react in the same way with several monosaccharides, incorporating them into the coordination sphere.

We will here show results of measurements performed on compounds formed by reaction between the complex ion cis-$[Co(NH_3)_4(H_2O)_2]^{3+}$ and the monosaccharides D-ribose, L-sorbose and D-glucosamine. These last were chosen considering the number of asymmetric carbon atoms per molecule, the series they belong to, and the presence of an amino group which has a good donor atom in the case of D-glucosamine (Fig. 1).

At the same time, studies in solution were carried out with the same Co(III) aminocomplex and other

carbohydrates in an attempt to find a correlation between the characteristics of the observed Cotton effects and their structure.
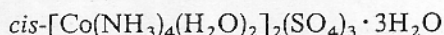
EXPERIMENTAL

Materials

The carbohydrates came from Merck and were used without further purification, but their $[\alpha]_D^t$ values were checked.

The complex cis-$[Co(NH_3)_4(H_2O)_2]_2(SO_4)_3 \cdot 3H_2O$ was synthesized in the laboratory following reported methods.[4]

Preparation of $[Co(NH_3)_4(D\text{-}ribose)]_2(SO_4)_3 \cdot 4H_2O$

A mixture of 0.835 g (1.25 mmole) of

$$cis\text{-}[Co(NH_3)_4(H_2O)_2]_2(SO_4)_3 \cdot 3H_2O$$

and 3.750 g (25 mmole) of D-ribose is dissolved in $25\ cm^3$ of water and the solution pH is adjusted to 6.2 with drops of ammonia solution. The temperature of
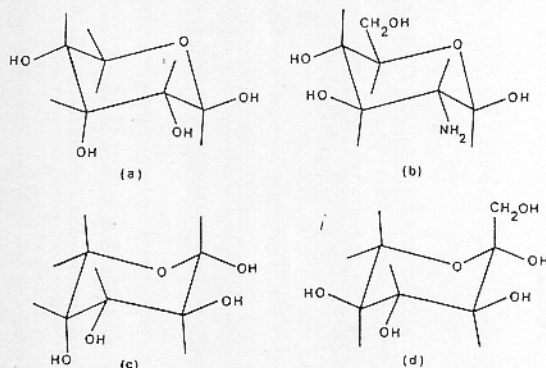

Fig. 1. (a) β-D-ribose; (b) β-D-glucosamine (2-amino-2-deoxy-D-glucose); (c) α-D-arabinose; (d) α-L-sorbose.

* Author to whom correspondence should be addressed.

the reacting mixture is kept at 30°C for 60 min in a thermoregulated water bath. A sample of the solution is placed in a thermostatted polarimetric cell of 0.5 cm pathlength and the course of the reaction is followed through the change of rotation of polarized light at 475 nm. Once the reaction stops the solution is removed from the bath and poured into a beaker, and 25 cm³ of methanol is added dropwise with constant stirring. The liquid is then centrifuged to eliminate traces of the polynuclear complex

$$[Co\{(OH)_2Co(NH_3)_4\}_3](SO_4)_3 nH_2O \ (n = 2-9),^5$$
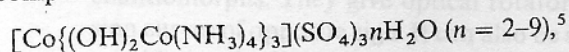
which is also formed in the course of the reaction and it was identified by analysis and IR spectrum. Methanol is then added to the clear solution with constant stirring up to a total addition of 100 cm³. During this process, the formation is observed of a microcrystalline precipitate which adheres to the walls of the beaker. The precipitate is separated by filtration in glass plates, washed with 5 cm³ methanol and then 5 cm³ ethanol; it is then quickly removed from the plate and dried under vacuum. The yield is about 350 mg.

The microcrystalline solid is deep pink, very soluble in water, giving a solution of the same colour. The solid compound is stable if kept in a dry atmosphere.

Found: C, 13.18; H, 5.48; N, 12.47; Co, 13.86; SO₄, 31.32. Calc: C, 13.13; H, 5.68; N, 12.25; Co, 12.91; SO₄, 31.51%.

Preparation of $[Co(NH_3)_4(L\text{-}sorbose)]_2(SO_4)_3$

0.835 g (1.25 mmole) of cis-$[Co(NH_3)_4(H_2O)_2](SO_4)_3 \cdot 3H_2O$ and 4.5 g (25 mmole) of L-sorbose are dissolved in 25 cm³ of water; the solution pH is raised to nearly 6.5 with drops of ammonia solution. The procedure previously described is followed, but in this case the maximum value of rotation is reached after 45 min of heating at 30°C. The yield is 400 mg.

The compound is a deep pink microcrystalline solid, stable in a dry atmosphere. It is soluble in water and the solutions decompose slowly. Dissociation of the complex species was checked by measuring the rotation of solutions prepared by successive dilutions.

Found: C, 15.49; H, 5.43; N, 12.67; Co, 14.3; SO₄, 32.63. Calc: C, 15.96; H, 5.32; N, 12.42; Co, 13.8; SO₄, 31.93%.

Preparation of $[Co(NH_3)_3(D\text{-}glucosamine)]_2 (SO_4)_3 \cdot 4H_2O$

A mixture of 0.835 g (1.25 mmole), of

$$cis\text{-}[Co(NH_3)_4(H_2O)_2]_2(SO_4)_3 \cdot 3H_2O$$
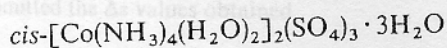
and 2.69 g (12.5 mmole) of D-glucosamine hydrochloride is dissolved in 55 cm³ of water; the solution pH is raised to 7 with drops of ammonia solution. The procedure described for the preparation of the complexes previously mentioned is applied with the following modifications: (a) the time needed to reach the maximum value of rotation at 475 nm is 40 min; (b) after addition of the first 25 cm³ of methanol to the solution and centrifugation, another 50 cm³ of the same solvent is added. Formation is observed of a viscous dark red product adhering to the walls of the beaker. The supernatant is then separated and residues of methanol and water are evaporated with an air current. The viscous material is redissolved in 3 cm³ of water and then poured, drop by drop, into 70 cm³ of 95% methanol containing about 100 mg NaClO₄. The liquid is constantly stirred during the process. The yield is 400 mg.

The compound is a violet microcrystalline solid, water soluble, giving deep red solutions. It is a stable compound in the absence of humidity.

Found: C, 15.47; H, 5.52; N, 12.01; Co, 12.45; SO₄, 31.36. Calc: C, 15.38; H, 5.55; N, 11.96; Co, 12.60; SO₄, 30.76%.

Analyses of C, H and N were performed with a Perkin–Elmer 240 microanalyzer. Carbon was also determined from the sugar content and analyzed by oxidation with ceric sulphate,[6] and nitrogen was checked as NH₃ with a specific electrode, after digestion with sulphuric acid.

Cobalt content was iodometrically determined as Co₂O₃.[7]

Sulphate analyses were carried out both gravimetrically and by means of a chloride-exchange resin in a column, the exchanged chloride being measured with an appropriate electrode.

Water of hydration was estimated by variation in whole number multiples to give best agreement with analytical data. Compounds with different number of hydration water molecules are obtained. Results herein reported correspond to one batch in each case. These variations in composition are reflected through bigger or smaller values of the measured optical activity.

Absorption spectra were measured with a Zeiss PMQ-2 spectrophotometer over 10^{-2} to 10^{-3} M solutions of the complexes.

Optical rotatory dispersion measurements were carried out with a modified Perkin–Elmer 141 polarimeter and Bausch and Lomb monochromator over 10^{-2} M water solutions using 2 cm pathlength cells. Variation of the angle of rotation against time was followed employing a 0.5 cm pathlength cell.

Circular dichroism measurements were carried out with a Schimadzu QV-50 spectrophotometer

fitted with circular dichroism attachment, on 10^{-2} M solutions with 1 cm pathlength cells.

RESULTS AND DISCUSSION

Figure 2 is shown as an example of the optical activity of the reaction product in solution between the Co(III) aminocomplex and D- and L-arabinose respectively, once the maximum value of rotation at one wavelength is reached in each case. These carbohydrates were chosen because they are enantiomorphs. They give optical rotatory dispersion curves of opposite sign. It can also be seen that, considering the dispersion curve of the carbohydrate as a base line, two Cotton effects are apparent in the region of Co(III) visible first absorption band. Maximum rotation is attained after 100 min.

The reagent cis-$[Co(NH_3)_4(H_2O)_2]^{3+}$ has two visible absorption bands: the first one is located at 505 nm and the second one at 355 nm. Introduction of carbohydrate into the coordination sphere causes a shift of the first absorption band maximum to 525 nm and of the second one to 375 nm. Besides, the second band is overlapped by an intense charge-transfer transition located at 220 nm with an extinction coefficient of 11,600 cm^2 $mole^{-1}$.

From the spectroscopic point of view, complexes of the type $[Co(NH_3)_4(carbohydrate)]^{3+}$ behave like the complex $[Co(NH_3)_4CO_3]^+$,[8] whose first and second absorption bands are located at 522 and 360 nm respectively. The spectra correspond, in both cases, to the coordination of 4 nitrogen and two cis-oxygen atoms around the Co(III) ion. Therefore the carbohydrate contribution would turn out to be similar to that of the carbonate ion.

In the complexes formed by D-ribose and L-sorbose the second absorption band keeps its identity (Table 1); but in the complex with D-glucosamine overlapping is broader and the second d–d band appears as only a shoulder at 375 nm.

The two Cotton effects with − + sign sequence observed in Fig. 3 are located under the first absorption band of the complexes formed by D-ribose, L-sorbose and D-glucosamine, in agreement with the two signals of opposite sign revealed by the circular dichroism spectra of the same compounds (Table 1).

This pattern of separation is characteristic of complexes of the type cis-$[Co(NH_3)_4L_2]$ where L is a

bidentate or a non-charged monodentate ligand. The $^1T_{1g}$ transition in C_{2v} symmetry is split in one component with A_2 symmetry and two others with B_1 and B_2 symmetries. The last two components generally intermix, whereas the A_2 state remains invariant.[9] Similar result is obtained under the holohedrized D_{4h} symmetry, where the $^1T_{1g}$ transition is split into the $^1A_{2g}$ and E_g transitions, which have an energy difference $\frac{1}{4}[\Delta_O - \Delta_{NH_3}]$. Considering that Δ_O (O = carbohydrate oxygen atom) is smaller than Δ_{NH_3}, it is possible to deduce that the negative circular dichroism component would correspond to the A_2 state, whereas the positive component would correspond to the E state.[10]

In all three cases the molar amplitudes of the Cotton effects centred at 510 nm are remarkably high: values range from 5900 to 13,350°. They are thus much higher than values given by a complex such as $[Co(NH_3)_4(sarcosinate)]^{2+}$, where the molar amplitude of the positive Cotton effect in the visible region is 1800°.[11]

The complexes formed by D-ribose and L-sorbose show only one positive circular dichroism signal in the charge-transfer spectral zone and they are placed at 300 and 320 nm respectively. The complex formed by D-glucosamine has two circular dichroism signals instead: a positive one at 315 nm and a negative signal at 270 nm.*

Taking account of the fact that the isolated compounds showed the same type of optical rotatory dispersion curve as that of the reaction products in solution, further experiments were performed with other carbohydrates and derivatives. They were selected so that they would permit the correlation of the sign of optical rotation of the complexes formed with the structure of the carbohydrate. In this way, the sign of the Cotton effect centred at 500 nm is positive for the product of the reaction between the tetramino Co(III) complex and 2-deoxy-D-glucose, whereas in the reaction product with α-methyl-D-glucoside the same is negative (Fig. 4).

The signs of the Cotton effects in the visible absorption region are the same for the compounds formed by D-ribose, L-sorbose, D-glucosamine and L-arabinose. This result is striking at first sight in view of the different configurations of these carbohydrates, the number of asymmetric carbon atoms and the possibilities of anomeric mixtures and pyranoidal or furanoidal structures. The constant pattern of optical rotatory dispersion in spite of the diversity of structural possibilities can be accounted for if one admits the requirement of a surrounding of identical chirality around the Co(III) ion in all these compounds.

It is well known that the anomeric equilibrium is

---

* Circular dichroism spectra in the UV region were measured in Santa Barbara, California with a Cary 60 spectropolarimeter. The complexes could have partially lost their optical activity on travelling; therefore we have omitted the Δε values obtained.
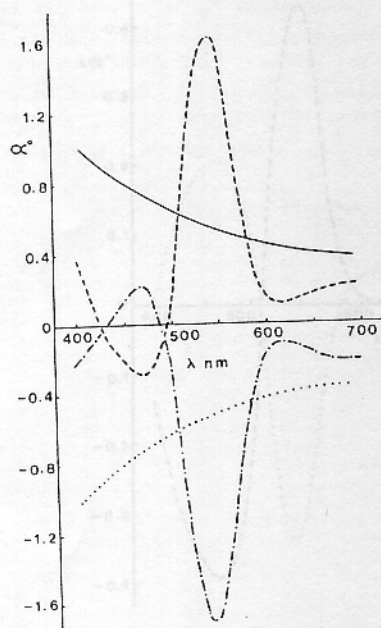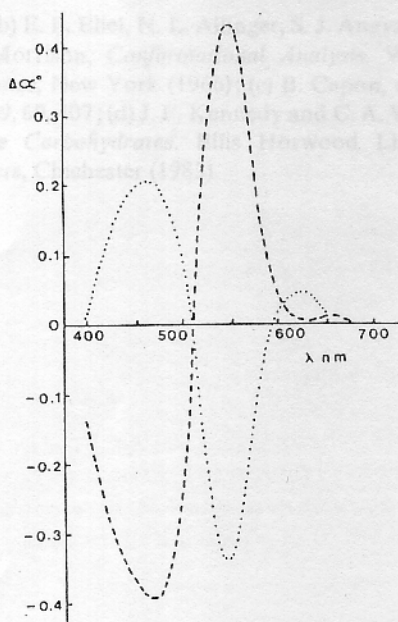
Fig. 2. Optical rotatory dispersion of complex species formed in solution after 100 min at 30°C, pH 6, 0.5 cm pathlength cell: (---) cis-[Co(NH$_3$)$_4$(H$_2$O)$_2$]$^{3+}$ 0.1 M/L-arabinose 0.5 M and (—·—·—) cis-[Co(NH$_3$)$_4$(H$_2$O)$_2$]$^{3+}$ 0.1 M/D-arabinose. Optical rotatory dispersion of: (——) L-arabinose 0.5 M and (····) D-arabinose 0.5 M.

shifted towards the β-form in the carbohydrates D-glucosamine and D-ribose; whereas D-arabinose is mainly an α-anomer.[12] Accepting that the carbohydrates bond to Co(III) preferably through the OH groups of C1 and C2, the chelate rings formed display an arrangement of one carbon atom over and another one under the xy plane of the {Co(NH$_3$)$_4$} species looked at from the metallic centre and moving from left to right, as can be appreciated in
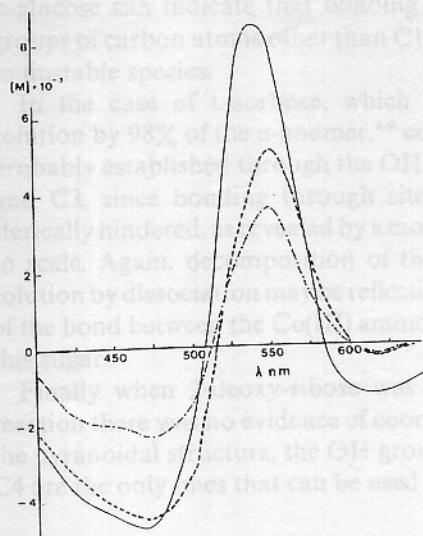
Fig. 3. Optical rotatory dispersion curves of the ions: (—·—·—) [Co(NH$_3$)$_3$(H$_2$O)(D-glucosamine)]$^{3+}$, (---) [Co(NH$_3$)$_4$(L-sorbose)]$^{3+}$ and (——) [Co(NH$_3$)$_4$(D-ribose)]$^{3+}$.

Fig. 5. This arrangement of atoms is somehow equivalent to the conformation adopted by the N–C–C–N chain of the ethylenediamine molecule when bonding to the Co(III) ion to form a complex.[13]

Besides the bonding sites already mentioned, other existing possibilities would lead to identical chiral ring, for example the OH groups of C3 and C4 of D-glucosamine; or else, the OH groups of C2 and C3 of D-ribose or of L-sorbose.

The preference for coordination through the donor groups bonded to C1 and C2 is perhaps reflected in the signs of the Cotton effects observed in the reaction product in solution of α-methyl-D-glucoside with the Co(III) aminocomplex, which are

Table 1. Visible-absorption and circular dichroism data

Complex species	Absorption		Circular dichroism	
	λ_{max} (nm)	ε_{max} (nm)	λ_{max} (nm)	$\Delta\varepsilon$
[Co(NH$_3$)$_4$(D-ribose)]$^{3+}$	530	94	570	−1.9
			505	2.9
	375	166	390	−1.6
[Co(NH$_3$)$_4$(L-sorbose)]$^{3+}$	530	81	570	−0.9
			505	2.2
	378	134	390	−1.0
[Co(NH$_3$)$_3$(H$_2$O)(D-glucosamine)]$^{3+}$	528	76	570	−0.9
			505	1.6
	375 (sh)	111	390	−0.8

Fig. 4. Optical rotatory dispersion of complex species formed in solution after 30 min at 30°C, pH 6, 0.5 cm pathlength cell. ($\cdots$) cis-[Co(NH$_3$)$_4$(H$_2$O)$_2$]$^{3+}$ 0.1 M/α-methyl-glucose 0.5 M; ($--$) cis-[Co(NH$_3$)$_4$(H$_2$O)$_2$]$^{3+}$ 0.1 M/2-deoxy-glucose 0.5 M. $\Delta\alpha = \alpha_{complex\,species} - \alpha_{carbohydrate}$.

opposite to those of the complexes containing D-ribose, L-sorbose and D-glucosamine. Structurally, coordination through sites 1 and 2 of the glucoside gives rise to a ring of the corresponding opposite chirality, although bonding to the metallic ion can also be achieved through the OH groups of C3 and C4.

When 2-deoxy-D-glucose is used for the reaction, the sign of the Cotton effect centred at 510 nm, is the same as that obtained for the complexes formed by D-ribose, L-sorbose and D-glucosamine. According to our proposal this is achieved by coordination through the OH groups of C3 and C4, which are the only sites properly arranged for chelation in this carbohydrate.

The difficulties we have found to isolate a solid compound from the reaction product with 2-deoxy-
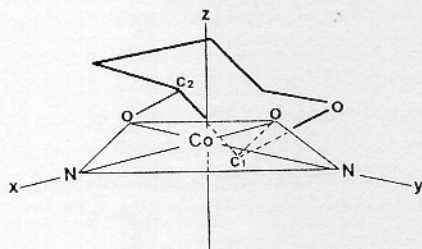
D-glucose can indicate that bonding through OH groups of carbon atoms other than C1 and C2 leads to unstable species.

In the case of L-sorbose, which is formed in solution by 98% of the α-anomer,[14] coordination is probably established through the OH groups of C2 and C3, since bonding through sites 1 and 2 is sterically hindered, as revealed by a molecular model to scale. Again, decomposition of the complex in solution by dissociation may be reflecting the lability of the bond between the Co(III) aminocomplex and this sugar.

Finally when 2-deoxy-ribose was used for the reaction there was no evidence of coordination. For the pyranoidal structure, the OH groups of C3 and C4 are the only ones that can be used for chelation.

Fig. 5.

REFERENCES

1. (a) S. J. Angyal, Chem. Soc. Rev. 1980, 9, 415; (b) C. C. Hinckley, P. S. Ostenburg and W. J. Roth, Polyhedron 1982, 1, 335; (c) S. J. Blunden, P. A. Cusack and P. J. Smith, Inorg. Chim. Acta 1983, 72, 217; (d) M. Tonković, O. Hadzija and I. Nagy-Czako, Inorg. Chim. Acta 1983, 80, 251; (e) A. Cervilla, J. A. Ramirez and A. Beltran-Porter, Transition Met. Chem. 1983, 8, 21; (f) T. Tsubomura, Sh. Yano and S. Yoshikawa, Polyhedron 1983, 2, 123.
2. O. Pavez, Tesis de Licenciatura, Facultad de Ciencias Básicas y Farmacéuticas, Universidad de Chile (1984).
3. O. Cisterna, Tesis de Licenciatura, Facultad de Ciencias Básicas y Farmacéuticas, Universidad de Chile (1984).
4. A. M. Greenaway and R. J. Lancashire, J. Chem. Educ. 1982, 59, 419.
5. G. Blyholder and N. Ford, J. Phys. Chem. 1964, 68, 1496.
6. N. N. Sharma, Anal. Chim. Acta 1956, 14, 423.
7. D. N. Grindley, An Advanced Course in Practical Inorganic Chemistry. Butterworths, London (1964).
8. V. S. Sastri and C. H. Langford, Can. J. Chem. 1969, 47, 4237.
9. A. J. McCaffery, S. F. Mason and B. J. Norman, J. Chem. Soc. 1965, 5094.
10. C. J. Hawkins, J. A. Stark and C. L. Wong, Aust. J. Chem. 1972, 25, 273.
11. D. A. Buckingham, S. F. Mason, A. M. Sargeson and K. T. Turnbull, Inorg. Chem. 1966, 5, 1649.
12. (a) J. Staneck, M. Cerny, J. Kocourek and J. Pacak, The Monosaccharides. Academic Press, New York

(1963); (b) E. L. Eliel, N. L. Allinger, S. J. Angyal and G. A. Morrison, *Conformational Analysis*. Wiley–Interscience, New York (1966); (c) B. Capon, *Chem. Rev.* 1969, **69**, 407; (d) J. F. Kennedy and C. A. White, *Bioactive Carbohydrates*. Ellis Horwood Limited Publishers, Chichester (1983).

13. (a) J. Corey and J. C. Bailar, *J. Am. Chem. Soc.* 1959, **81**, 2690; (b) G. Snatzke, *Optical Activity and Chiral Discrimination* (Edited by S. F. Mason). Reidel Publishing Company, Dordrecht (1978).

14. W. Funcke and C. von Sonntag, *Carbohydr. Res.* 1979, **75**, 305.

Figura 22: *Línea de polimerización de etileno.*

Figura 23: *Flowsheet de la línea de polimerización de etileno.*

Un resumen de las reacciones de copolimerización se presenta en la Tabla 4.3. Cada variable corresponde a un promedio de los resultados de tres reacciones idénticas.

La polidispersidad resultó entre 1,8 and 2,0, valores comúnmente encontrados en polímeros metalocénicos[35].

Tabla 4.3: Efecto de la concentración y tipo de comonómero en las propiedades de copolímeros isotácticos, obtenidos utilizando el catalizador $Me_2Si(2\text{-}Me\text{-}Ind)_2ZrCl_2$

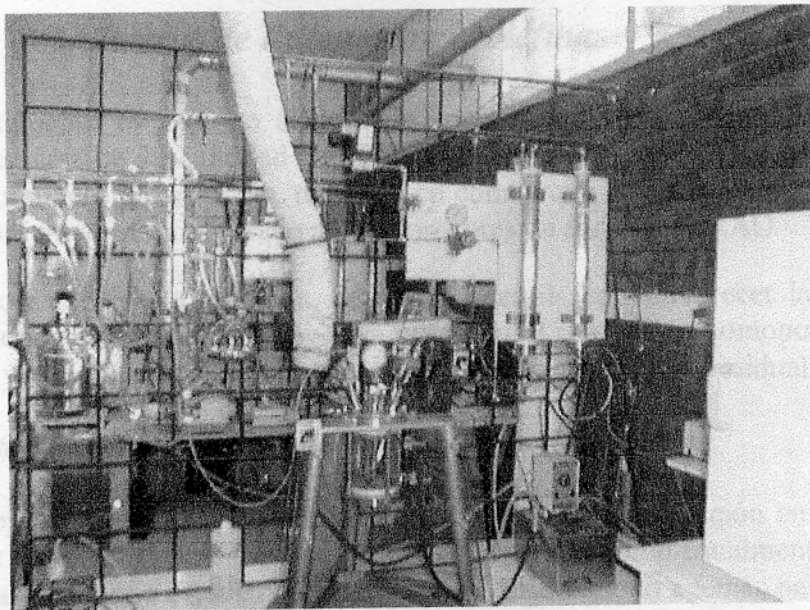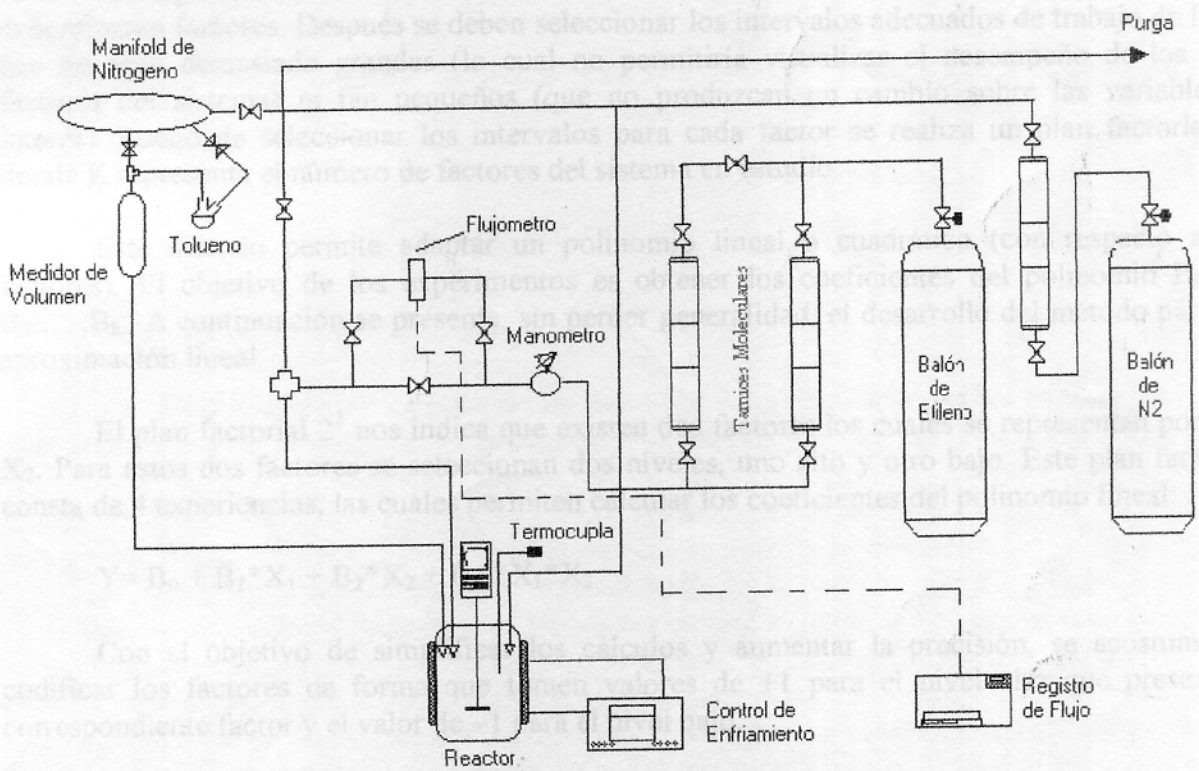| Muestra	Comonómero	Concentración comonómero (mol/L)	Actividad (kg/mol Zr/ bar/h)	$\overline{M}_w$ (kg/mol)	Incorporación (% molar)	fc	Tm (ºC)	ΔH_m (J/g)
PPI	-	0,00	15.000	201	0,0	0,45	152	95
PPI-H4	1-hexeno	0,13	16.300	154	2,2	0,32	131	67
PPI-H1	1-hexeno	0,32	15.700	129	5,6	0,24	109	50
PPI-H2	1-hexeno	0,60	18.300	122	9,0	0,11	86	24
PPI-H3	1-hexeno	0,90	13.300	141	12,0	0,10	60	20
PPI-O4	1-octeno	0,13	17.400	142	2,2	0,40	128	85
PPI-O1	1-octeno	0,32	19.200	141	5,6	0,17	98	35
PPI-O2	1-octeno	0,60	15.600	112	7,2	0,07	80	15
PPI-O3	1-octeno	0,90	12.800	130	13,3	0,06	46	12
PPI-D1	1-deceno	0,13	14.000	190	0,2	0,48	149	100
PPI-D2	1-deceno	0,32	11.900	154	0,6	0,47	142	99
PPI-D3	1-deceno	0,60	12.700	144	1,0	0,48	136	100
PPI-Do1	1-dodeceno	0,13	11.100	179	2,9	0,26	122	55
PPI-Do2	1-dodeceno	0,32	12.000	163	4,6	0,17	96	36
PPI-Do3	1-dodeceno	0,60	9.300	151	9,3	0,06	71	13
PPI-Do4	1-dodeceno	0,90	8.000	133	12,7	nd	45	nd
PPI-T1	1-tetradeceno	0,13	12.400	154	2,6	0,25	124	52
PPI-T2	1-tetradeceno	0,32	9.000	134	4,7	0,17	98	36
PPI-T3	1-tetradeceno	0,60	6.500	121	9,2	0,03	75	7
PPI-OD1	1-octadeceno	0,13	28.200	170	1,9	0,34	129	70
PPI-OD2	1-octadeceno	0,32	24.600	159	3,7	0,04	103	9
PPI-OD3	1-octadeceno	0,60	19.400	146	8,0	0,09	53	19

Condiciones de reacción: presión de propileno (relativa): 2 bar; moles de Zr en el reactor = 5×10^{-6}; [Zr] = 10×10^{-6} mol/L; Al/Zr =1.000; T= 45 °C; tiempo de reacción = 30 min. (nd: valor no disponible).

4.1.3.1. Incorporación de Comonómero

La incorporación de comonómero fue determinada por ^{13}C-RMN.

A modo de ejemplo, en las Figuras 4.2 y 4.3 se presentan los espectros de PP isotáctico y del copolímero con 1-hexeno con 12% molar de incorporación, respectivamente. En la Figura 4.2 aparecen las tres señales intensas características del PP: la señal en 21 – 22 ppm, que corresponde al carbono del sustituyente metil (CH_3); el pico en 28 – 28,5 ppm, que corresponde al átomo de carbono terciario (α-CH), que está sustituido por el grupo metilo; y aquella relacionada con el grupo β-CH_2 de la cadena principal, en 46 - 47 ppm.

La señal de α-CH se utiliza como referencia para el cálculo de incorporación de comonómero. En la Figura 4.3, la señal en 33,4 ppm se asocia con el grupo –CH$_2$- de una ramificación aislada[74]; la señal en 35 – 35,5 ppm se relaciona con la presencia de una ramificación, es decir, de un átomo de carbono terciario sustituido por una cadena de n carbonos (n > 4)[75].

Para todos los comonómeros estudiados fue posible incorporar comonómero en la cadena polimérica. Existe una relación prácticamente lineal entre el porcentaje molar de comonómero incorporado en el polímero y la concentración de comonómero en el reactor, para todos los comonómeros, como se observa en la Figura 4.4. El 1-deceno, si bien exhibe la misma tendencia lineal, presenta incorporaciones mucho más bajas en comparación con los otros comonómeros.

Considerando todos los comonómeros, excepto el 1-deceno, se ha ajustado la ecuación de una recta (ecuación 4.2) para relacionar la incorporación de comonómero en la cadena con la concentración de comonómero en el reactor:

$$\text{Incorporación (\% molar)} = 13,304 \times \text{concentración (M)} + 0,6605 \qquad [4.2]$$

El factor de correlación de 0,97 indica una buena calidad del ajuste.

Considerando solamente los copolímeros propileno/ 1-deceno, se ha obtenido una ecuación similar (ecuación 4.3), con un factor de correlación de 0,99:

$$\text{Incorporación (\% molar)} = 3,5866 * \text{concentración (M)} + 0,0085 \qquad [4.3]$$
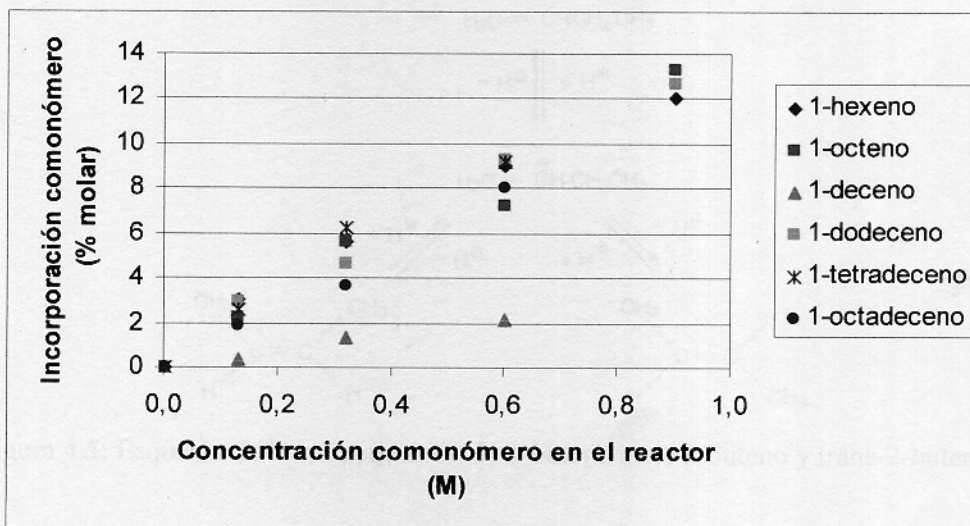
Figura 4.4: Dependencia de la incorporación de comonómero en el polímero
isotáctico con la concentración de comonómero en el reactor.

La incorporación de deceno corresponde a un valor entre 75% y 85% del valor de incorporación promedio de los otros comonómeros, a concentraciones similares en el reactor. No se encuentra una explicación convincente para este fenómeno, ya que en literatura no se ha encontrado reportada una dificultad adicional para la copolimerización de 1-deceno con propileno, ni

Tabla 4.5: Efecto de la incorporación de comonómero en la tacticidad del
copolímero (tacticidad basada en las diadas)

| Muestra	Comonómero	Concentración comonómero (mol/L)	Incorporación (% molar)	Tacticidad
PPI	-	0,00	0,0	98,0
PPI-H4	1-hexeno	0,13	2,2	98,6
PPI-H1	1-hexeno	0,32	5,6	97,0
PPI-H2	1-hexeno	0,60	9,0	97,4
PPI-H3	1-hexeno	0,90	12,0	97,0
PPI-O4	1-octeno	0,13	2,2	97,0
PPI-O1	1-octeno	0,32	5,6	98,1
PPI-O2	1-octeno	0,60	7,2	95,1
PPI-O3	1-octeno	0,90	13,3	95,0
PPI-D1	1-deceno	0,13	0,2	97,5
PPI-D2	1-deceno	0,32	0,6	97,4
PPI-D3	1-deceno	0,60	1,0	96,9
PPI-Do1	1-dodeceno	0,13	2,9	96,9
PPI-Do2	1-dodeceno	0,32	4,6	97,2
PPI-Do3	1-dodeceno	0,60	9,3	97,4
PPI-Do4	1-dodeceno	0,90	12,7	97,2
PPI-T1	1-tetradeceno	0,32	4,7	96,0
PPI-T2	1-tetradeceno	0,60	9,2	97,3
PPI-OD1	1-octadeceno	0,13	1,9	97,3
PPI-OD2	1-octadeceno	0,32	3,7	95,5
PPI-OD3	1-octadeceno	0,60	8,0	97,7
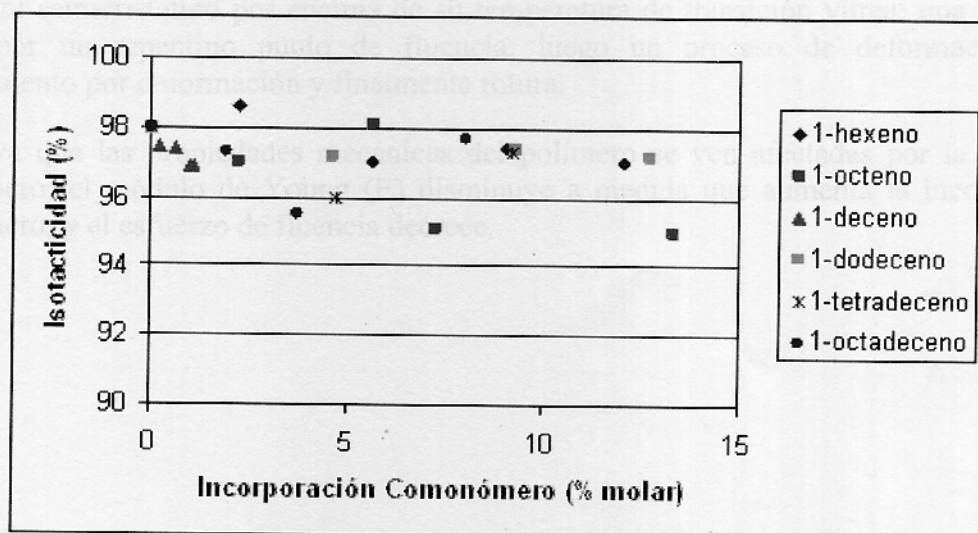
Figura 4.19: Efecto del comonómero en la tacticidad para copolímeros isotácticos.

4.1.3.5. Propiedades Mecánicas

Se realizaron ensayos de tracción - deformación al homopolímero y a los copolímeros con diferentes incorporaciones de 1-hexeno y de 1-octeno. Sólo fueron ensayados los copolímeros con estas dos α-olefinas pues se considera que todos los comonómeros presentan una tendencia similar en este tipo de ensayo mecánico[85,86]. Además, tanto 1-hexeno como 1-octeno, por ser de cadena más corta, tienen posibilidad de ser utilizados comercialmente como comonómeros en la polimerización de olefinas.

Como mínimo unas cinco probetas de cada material fueron ensayadas; el espesor de las probetas fue del orden de 0,2 a 0,3 mm, y la velocidad el ensayo, 50 mm/min. Los resultados se presentan en las Tabla 4.6 y 4.7.

Tabla 4.6: Propiedades mecánicas de PP isotáctico y copolímeros con 1-hexeno

Muestra	Incorporación hexeno (% molar)	E (MPa)	Fluencia		Rotura	
			Esfuerzo (MPa)	Elongación (%)	Esfuerzo (MPa)	Elongación (%)
PPI	-	979	36	8	28	248
PPI-H4	2,2	656	25	10	30	443
PPI-H1	5,6	408	15	11	32	455
PPI-H2	9,0	190	6	15	28	594
PPI-H3	12,0	71	4	13	22	546

La Figura 4.20 muestra las curvas esfuerzo – deformación para PP homopolímero isotáctico y copolímeros de propileno con 1-hexeno. El homopolímero muestra el comportamiento típico de un material semicristalino por encima de su temperatura de transición vítrea: una zona elástica seguida por un repentino punto de fluencia, luego un proceso de deformación en frío, endurecimiento por deformación y finalmente rotura.

Se observa que las propiedades mecánicas del polímero se ven afectadas por la presencia de comonómero: el módulo de Young (E) disminuye a medida que aumenta la incorporación de comonómero, y el esfuerzo de fluencia decrece.

Tabla 4.7: Propiedades mecánicas de PP isotáctico y copolímeros con 1-octeno

Muestra	Incorporación octeno (% molar)	E (MPa)	Fluencia		Rotura	
			Esfuerzo (MPa)	Elongación (%)	Esfuerzo (MPa)	Elongación (%)
PPI	-	979	36	8	28	248
PPI-O1	2,2	648	25	9	29	430
PPI-O1	5,6	267	13	9	28	311
PPI-O2	7,2	84	6	9	23	485